Kochi Chapter

Indian Geotechnical Conference
IGC 2022
15th – 17th December, 2022, Kochi

3-Dimensional Finite Element Analysis of Shankumugham Beach Road Due To Rainfall-Induced Storm Surge

Parvathi G. S.[1], Mariya Dayana P. J.[2], Anil Kumar Sinha[3], Vasant G Havanagi[4]

[1] Senior Scientist, Geotechnical Engineering Division, CSIR- Central Road Research Institute, Delhi- 110025, parvathi.crri@nic.in
[2] Scientist, Geotechnical Engineering Division, CSIR- Central Road Research Institute, Delhi- 110025, mdpj.crri@nic.in
[3] Senior Principal Scientist, Geotechnical Engineering Division, CSIR- Central Road Research Institute, Delhi- 110025, sinha.crri@nic.in
[4] Chief Scientist, Geotechnical Engineering Division, CSIR- Central Road Research Institute, Delhi- 110025, vasant.crri@nic.in

Abstract. Over the past few years, heavy rainfall-induced storm surge has resulted in coastal erosion and consequent beach loss in Kerala. Shankumugham beach road in the Thiruvananthapuram district is one such road that was earlier protected by a gabion wall along the seashore. During the 2019/2020 monsoon period, the gabion walls and half lane of the road got washed away due to rainfall-induced storm surge. Due to heavy rainfall, the tidal height increased by 21% which led to the erosion of beach soil, including the foundation soil of the gabion wall. To reclaim the beach road, remedial measures in the form of a diaphragm wall with rubble mound and soil anchor were designed and constructed. In the present study, a 3-dimensional finite element modeling (FEM) of the diaphragm wall and armor layer was performed considering the dynamic effects of wave action. In addition, a comparative study was done between the 2D limit equilibrium method (LEM) analysis result and the 2D and 3D FEM output under static and dynamic loading conditions. The results from the study verify the stability of the structure in the existing condition.

Keywords: Diaphragm wall, Coastal, Mitigation, Wave dynamics.

1 Introduction

Kerala's shorelines are under constant threat during the monsoon season due to coastal erosion. The adverse influence of climatic changes results in the alteration of the shoreline of the coast (Davis and FitzGerald 2009; Erlandson 2012). Shankumugham is one such shoreline located in the Thiruvananthapuram district of Kerala, India. The shore of this beach is very gentle (10° horizontal). A two-lane road runs parallel to this shoreline. Initially, a 1.5m high gabion wall facing the seaside retained the road. In 2019/2020 due to constant wave activities especially during monsoon, the gabion structure failed due to coastal erosion. Along with the gabion wall, half the carriageway width of the road was washed away. The destruction continued in 2021, damaging the remaining road as shown in Fig 1. The traffic was reinstated in 2022 by constructing a diaphragm wall with soil anchor and rubble mound to safely re-erect the road.

Fig. 1. Shankumugham Beach Road

The authors of the paper have published a detailed case study of the Shankumugham road failure and mitigation measures adopted (Sreekantan et al., 2022), where safety analysis of the recommended structure was reported. In that study, conventional Limit Equilibrium Method (LEM) were adopted for analysis for varying water levels to stimulate the worst field condition. The dynamic sea wave energy acting on the structure was converted to static force and moment for the analysis. Considering the importance of the structure and the dynamicity involved, the present study analyzes the stability of the structure using 3-Dimensional (3D) Finite Element Modeling (FEM) under rainfall-induced wave dynamic force. To this end, the site conditions from 2018 to 2022 were elaborated followed by deriving the design parameters for the FEM model development. 2D and 3D FEM models were developed considering the equivalent static as well as the dynamic tidal loading conditions. Stability of the structure is evaluated from the modelling output and compared with the LEM results reported by Sreekantan et al. (2022).

2 SITE CONDITION

Shankumugham beach road is an undivided two-lane pathway located along the seashore of Shankumugham beach. In the beginning, 1.5m high gabion walls were constructed along the seaside of the beach road to protect it against the sea waves. The gabion wall had an inverted ‘T’ shape with a 1.5m bottom width and 0.5m embedment below the shore level. The finished road level (FRL) was in line with the gabion top. The gabion wall was stable and functioned well until 2018 when the shore witnessed immense coastal erosion.

Shankumugham beach witnessed significant coastal erosion during the monsoon period. In a century, Kerala experienced an abnormally high rainfall in the 2018 monsoon (Vishnu et al. 2019). Considering this, both rainfall and tidal data were collected for the 2018–2019 period from the Indian Meteorological Department (IMD), India. The variation of maximum observed rainfall from January 2018 to October 2019 at Thiruvananthapuram is shown in Fig. 2. During this time period, August had the highest rainfall, with precipitation of 125mm (2018) and 97mm(2019) respectively. This was followed by the months of May (88.4mm, 2019) and September (88.6mm, 2019 & 79.8mm, 2018). The continuous rainfall with adverse climatic factors induced storm surges near the beach. The variation of tidal height during this period is shown in Fig. 3. The tides displayed their maximum height during the months of May to August corresponding to the highest rainfall period. This concludes that as precipitation increases, the height of the tidal wave increase. In 2018, a 21% increase in average tidal height was observed compared to the previous year. The maximum height was attained up to 0.511m in June 2018.

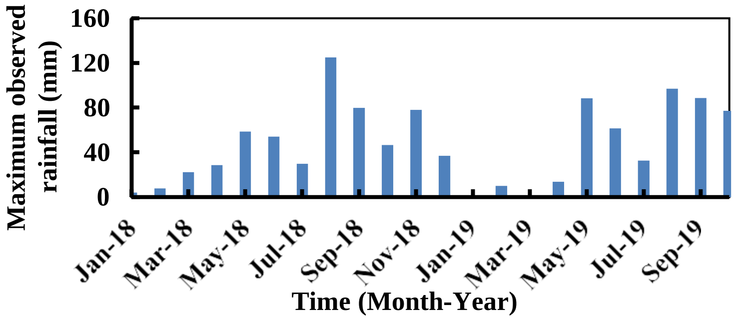

Fig. 2. Rainfall variation with time in Thiruvananthapuram

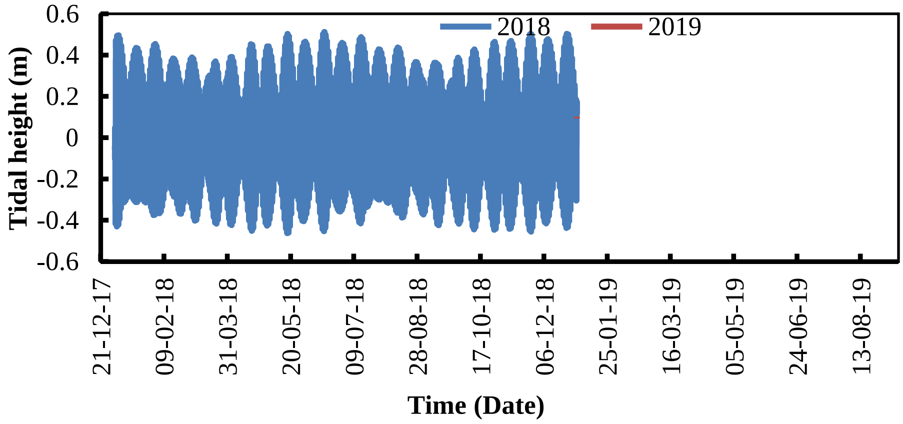

Fig. 3. Tidal height variation with time in Shankumugham Beach

In addition, the increase in storm surge is also related to the seawater depth. As the depth of seawater decreases, the storm surge increases. Therefore, the increased precipitation during monsoon in a gentler seabed like Shankumugham beach resulted in tidal height rise than normal. The Probable Maximum Storm Surge (PMSS) is about 3 m near Thiruvananthapuram coastal belt (BMTPC, 2019). This rise in tidal height increases the maximum wave uprush limit and expands the shoreline landwards. The variation in shoreline due to this phenomenon is shown in Fig. 4. The gap between shoreline and road edge shrunk from 42m in August 2016 to nearly 0m in August 2019. Thus, the increased storm surge with depleting shoreline width in monsoon resulted in coastal erosion, destabilizing the gabion wall, and subsequent failure for a stretch length of 260m.

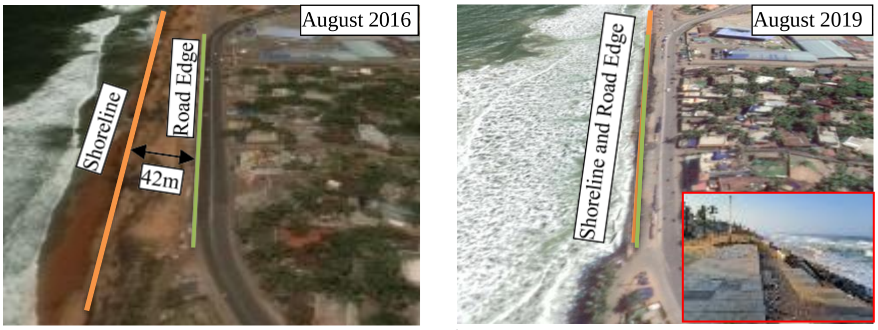

Fig. 4. Shoreline transformation with time

To stabilize the condition, an 8m deep diaphragm wall was constructed in 2022 to protect the road from further damage. The diaphragm wall was constructed along with soil anchoring to provide stability to the structure. The diaphragm wall and anchor was designed as per IS 9556(2003) and IS 10270 (2003). The anchor was positioned 1m below the diaphragm top evaluating the safety of the structure as well as the construction feasibility. Although the diaphragm wall with soil anchor could withstand the wave force, a 4m high rubble mound was constructed in front of the wall to reduce the wave force and scouring effect. The details of the section are shown in Fig. 5.

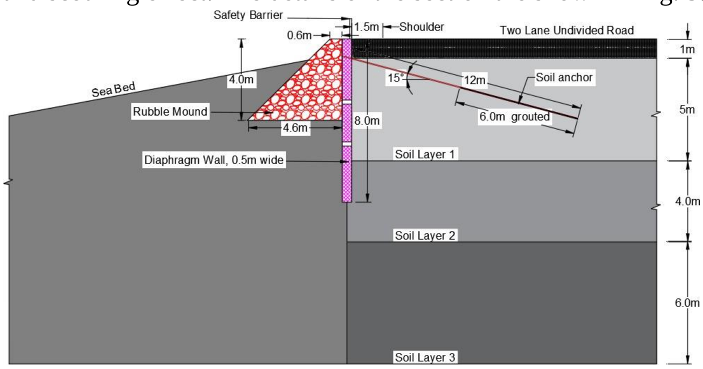

Fig. 5. Cross-section details of diaphragm wall with soil anchor and rubble mound

Sreekantan et al. (2022) analyzed the stability of the structure using 2-Dimensional (2D) LEM-based software. The structure was designed to withstand the in-situ stresses, traffic load (12kPa), and wave action. The dynamic effect of the wave was applied as static force (1.6kN) and moment (0.26kNm) in the model. Being on the seaside under shifting rainfall conditions, the site may experience varying water levels throughout the year. Therefore, the stability of the structure was analyzed for different construction stages by varying the scour depth (up to 4m) and water levels.

Although the reported factor of safety (FoS) from the 2D LEM analysis was adequate, it is essential to analyze this complex structure in FEM software under dynamic loads to reassure the safety of the structure. Therefore, a comparative study has been conducted between 2D LEM results and 2D & 3D FEM outputs. The details of modelling and their results are discussed as follows.

3 MODELING

Both 2D and 3D FEM finite element numerical modeling was carried out using MIDAS GTS NX software. AutoCAD interface of the software was used to model the geometry. For the 2D model, the geometry was created in the XY plane similar to the LEM study. While the 3D model was developed by creating a 2D geometry in the XZ plane and extruding the geometry 100m in Y-direction. For proper node-to-node connection, the common edges and surfaces were auto-connected using the auto-connect command in the software. Soil anchor was modeled as a linear element of length 12m and inclination 15° at 1m depth from the diaphragm top. In the 3D model, this linear element was translated at 1m spacing along the longitudinal direction (Y-axis). The material properties adopted for the models were detailed in Table 1 & 2.

Table 1. Design parameters

Layer	Bulk Density (kN/m^3)	Saturated Density (kN/m^3)	Cohesion (kpa)	Angle of Friction (deg)	Modulus of Elasticity (MPa)
Subgrade	18	19	1	35	28
Layer 1	16	17	1	25	10
Layer 2	18	18	1	32	20
Layer 3	18	18	1	35	25
Rubble mound	20	20	15	40	50

Table 2. Design parameters of diaphragm wall and soil anchor

Item	Material	Dimension	Model Type		Prestress load (kN)
			2D Model	3D Model	
Diaphragm wall	Concrete	100mx 0.5mx 8m (LxWxH)	1D Beam	2D Shell	-
Soil Anchor	Mild Steel	15mm(Dia.) 12m(length)	1D Embedded Truss		50

Properties remain the same, but materials were defined differently in 2D and 3D models. In the case of the 2D model, the sub-strata are defined as 2D plain strain elements while it is 3D solid elements in the 3D model. Similarly, the diaphragm wall is defined as a 1D beam element in the 2D model while it is a 2D shell element in the 3D model. However, in either of the cases, soil anchors are defined as 1D embedded truss elements. Based on these material definitions, meshing was done accordingly.

Six noded triangular elements of 0.5m size and fifteen noded tetrahedron elements of 1m size were used for the surface discretization of 2D and 3D models respectively, as shown in Fig. 6. Typically, the stresses developed in the soil anchor are transferred to the surrounding firm strata via the fixed length of soil anchor. This can be stimulated by controlling the mesh size. The lower the mesh size, the higher the node-to-node contact and the better the stress transfer. Accordingly, the initial 6m length (un-grouted) was meshed to generate two nodes, one at the start and one at the end. The remaining

6m (grouted) was meshed by dividing the 1D element into 10 divisions, to develop an adequate node-to-node contact with the surrounding soil.

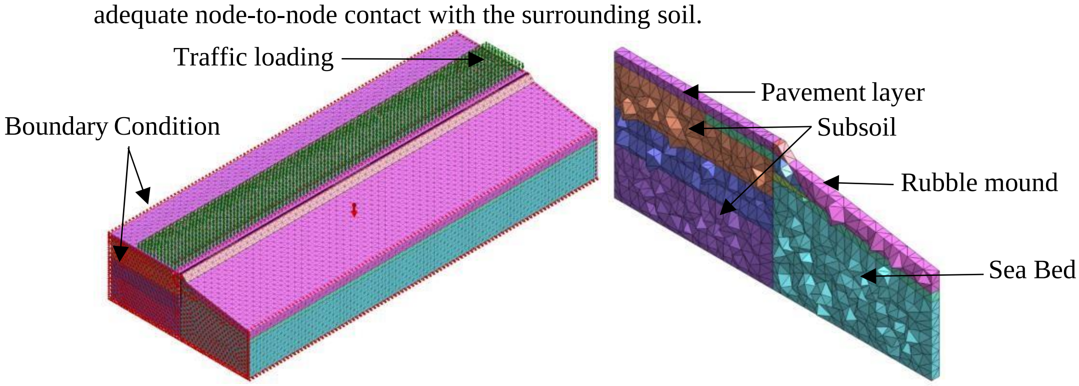

(a) 3D meshed model (b) Transverse-section of 3D mesh

Fig. 6. Shear Stress Contour Mapping

The mesh generation was followed by defining the loading conditions. Self-weight was defined initially for all cases. In static analysis, 24kPa traffic load was applied over the road top as a line load in 2D and as a pressure load in the 3D model study. Similarly, the wave force 1.6kN was applied at the 2/3rd height of the exposed wall as point load in the 2D model and as line load in the 3D model respectively.

In dynamic analysis, dynamic effects of traffic as well as tide were simulated simultaneously. Thus, the traffic load was converted into mass using live load to mass function. The tidal force was applied as a dynamic load to the structure. The wave force was computed using equation 1 (Deo 2013)

$$Total\ Force = P_s + P_d = \frac{\gamma}{2} d_b h_c \left(1 - \frac{x_1}{x_2}\right)^3 + \frac{1}{2}\gamma h_c^2 \left(1 - \frac{x_1}{x_2}\right)^2 \quad (1)$$

where P_s is the static force; P_d is the dynamic force; h_c is the height of wave above sea level; d_b is the depth of seabed from the SWL at breaking point = 1.4 xh_c; x_1 is the horizontal distance from the shoreline to embankment crest = 2 m; x_2 is the horizontal distance from the shoreline to maximum wave uprush limit = $2H_b/\tan\alpha$ = 11 m; and γ is the density of seawater = 10 kN/m^3.

To analyze the worst condition, the tidal data of the day corresponding to the maximum experienced tidal force was selected and this happens to be 15th June 2018. The time-varying tidal force is shown in Fig. 7. It shall be noted that the tidal force so obtained is found to be insignificant in comparison to the pavement loading and earth pressure acting on the structure. Where the soil anchor was modeled, a prestress load of 50kN was applied in the initial 6m free length of the anchor. The boundary condition was applied using the auto-constraint option, where the horizontal movements were restricted all around the sides whereas, both horizontal and vertical movements were restrained at the base of the model.

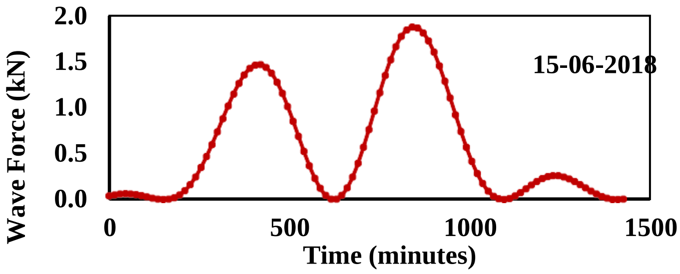

Fig. 7. Dynamic wave force variation with time

Static analysis was carried out for four construction stages in 2D, and 3D interfaces as shown in Fig. 8. In addition, slope stability analysis using the Strength Reduction Method (SRM) was also performed for all stages and the factor of safety was obtained. Considering the complexity of the structure and the number of load points involved in dynamic loading, the dynamic analysis was performed only for the completed structure i.e., Stage 3. A non-linear time history analysis was chosen for the analysis.

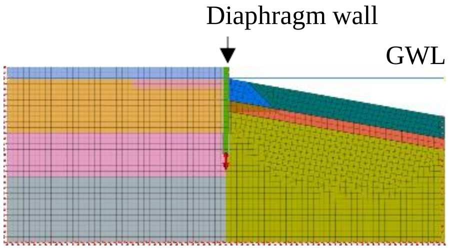

(a) **Stage 1**: Only diaphragm wall with scouring depth of 1 m (no pavement surcharge & 1m GWL on either side)

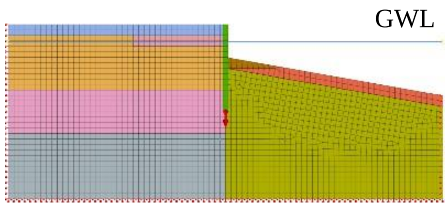

(b) **Stage 2**: Only diaphragm wall with scouring depth of 3 m (no pavement surcharge & 1m GWL on either side)

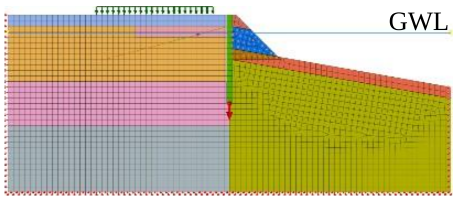

(c) **Stage 3**: Diaphragm wall with a soil anchor and rubble mound and scour depth of 3 m (With pavement surcharge 24kPa and GWL 1.6 m in front and behind the wall)

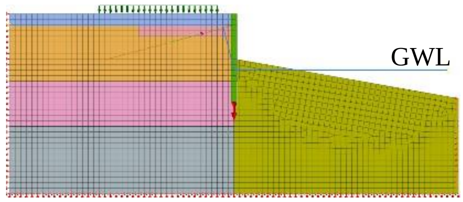

(d) **Stage 4**: Diaphragm wall with a soil anchor and no rubble mound with a scouring depth of 4 m (With pavement surcharge 24kPa and GWL 5.0 m in front and 1.0 m behind the wall)

Fig. 8. Construction stages for static analysis

4 RESULTS AND DISCUSSIONS

4.1 Static Analysis

The stability of a structure is defined by its factor of safety. The factor of safety obtained for all four construction stages in 2D, and 3D FEM analysis are compared with the 2D LEM study as shown in Fig. 9. In all three analyses, the variation in FoS is parallel. It is the highest in Stage 1, when the scour depth is only 1m in front of the diaphragm wall and decreased substantially in Stage 2 with an increase in scour depth by 2m. In Stage 3, although the scour depth was further increased by 1m, the FoS increased considerably due to the presence of a rubble mound in front of the structure. Stage 4 was analyzed to stimulate the worst-case scenario when the rubble mound is washed away, and water level difference occurs near the structure with a 4m scour depth. Soil anchor was introduced with a prestress load of 50kN, and the factor of safety attained met the codal requirements (IRC 75, 2015). It is interesting to note that the FoS attained in 2D FEM is less than the 2D LEM and 3D FEM output. The 3D FEM results are more realistic and found to be in good agreement with the LEM results as reported by Sreekantan et al. (2022).

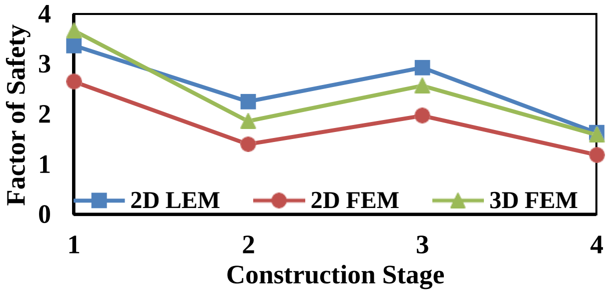

Fig. 9. Construction stage wise factor of safety variation

The shear stress contour developed for each case in 2D, and 3D model study is shown in Fig. 10. Due to plain strain conditions, the stress contour developed from the 3D analysis is an extruded version of the 2D result. In stage 1 and stage 2, the slip surface was formed narrow, while it is wide in stage 3 and stage 4. In stage 3 and stage 4, due to prestressing of the soil anchor, distress is observed to be transmitted to the pavement surface. This is in good agreement with the field observation wherein pavement distress was reported during anchor installation. A longitudinal and transverse view of the 3D output for Stage 4 is shown in Fig. 11. The symmetry indicates the plain strain property of the section.

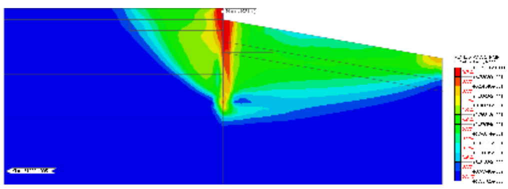

(a) 2D Model-Stage 1

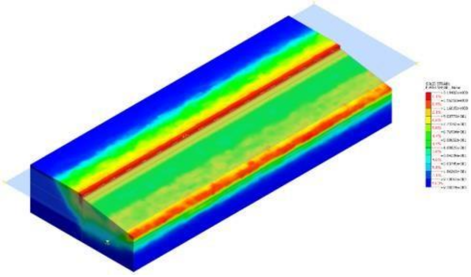

(b) 3D Model-Stage 1

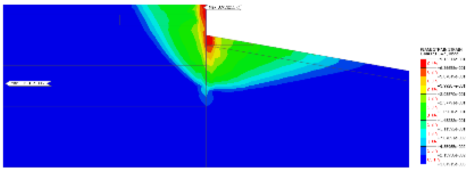
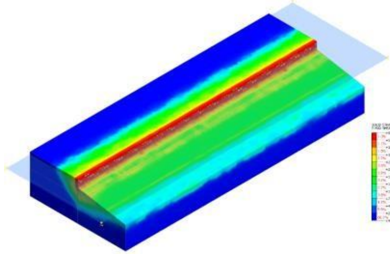

(c) 2D Model-Stage 2 (d) 3D Model-Stage 2

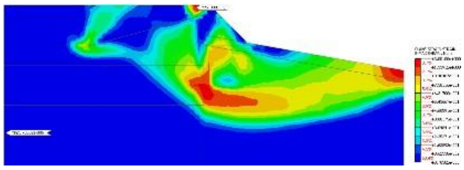
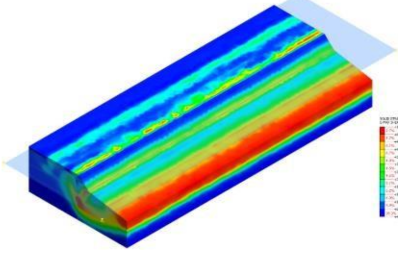

(e) 2D Model-Stage 3 (f) 3D Model-Stage 3

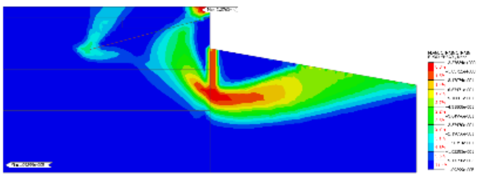
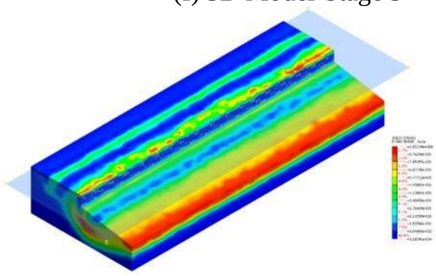

(g) 2D Model-Stage 4 (h) 3D Model-Stage 4

Fig. 10. Shear Stress Contour Mapping

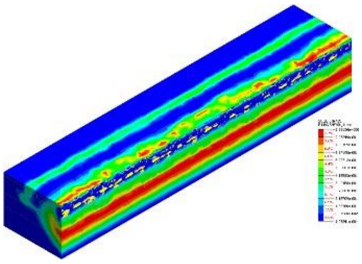
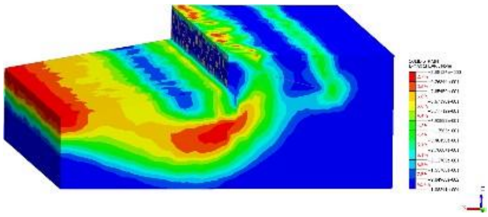

(a) Longitudinal section along Diaphragm wall (b) Transverse section at the centre of the alignment

Fig. 11. Cross-sectional detailing of 3D Model-Stage 4

The vertical displacement contour for each construction stage is shown in Fig. 12. Similar to shear stress, the displacement contours developed from 2D and 3D analysis are the same with a marginal difference in values. The maximum vertical settlement in the 2D model from Stage 1 to Stage 4 is found as 0 mm, -7 mm, -22 mm, and -39 mm respectively. While in the 3D model, it is 0mm, -4mm, -20mm, and -31mm respectively. In all cases, the vertical settlement is maximum near the landward side of the diaphragm wall, while the upheaval is observed at the seaside, both being negligible. A schematic view of the deformed shape of the structure after Stage 3 analysis is shown in Fig. 13. In stage 3, representing the existing condition of the structure, the maximum axial force developed in the soil anchor is 39kN in the 2D model and 44kN in 3D respectively. In either case, it is within the prestress force of 50kN. The axial force variation along the length of the soil anchor is shown in Fig. 14.

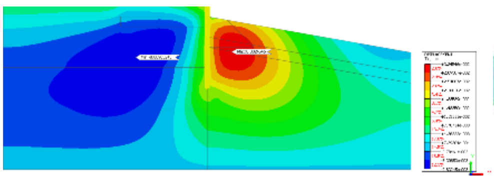

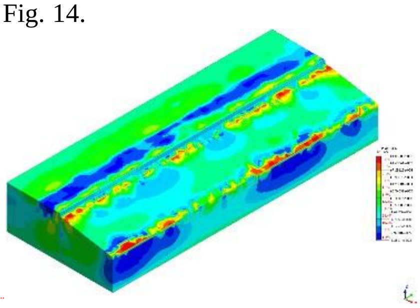

(a) 2D Model-Stage 1

(b) 3D Model-Stage 1

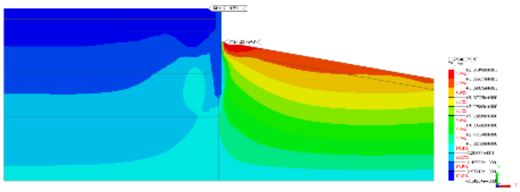

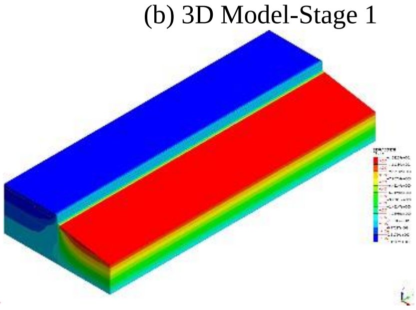

(c) 2D Model-Stage 2

(d) 3D Model-Stage 2

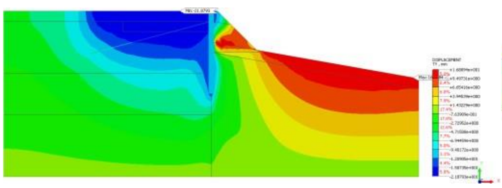

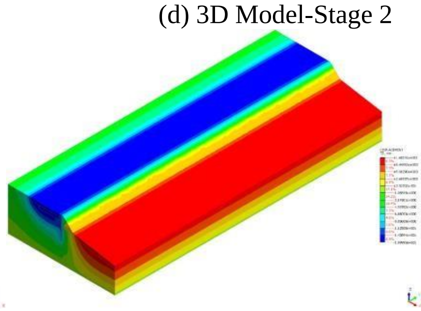

(e) 2D Model-Stage 3

(f) 3D Model-Stage 3

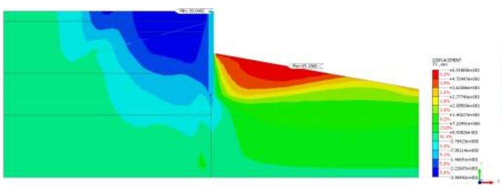

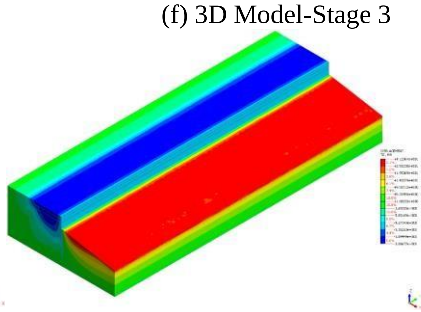

(g) 2D Model-Stage 4

(h) 3D Model-Stage 4

Fig. 12. Vertical displacement contour mapping after static analysis

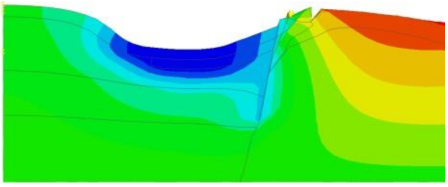

Fig. 13. Exaggerated deformed shape of the structure - Stage 3

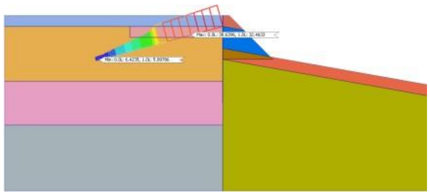

Fig. 14. Axial force developed in 2D Model-Stage 3

4.2 Dynamic Analysis

A 2D and 3D dynamic analysis was performed for the existing condition of the structure (Stage-3). A scour depth of 3m was taken based on theoretical calculation (Fowler, 1993) and field observations. Like the static case, the outputs from 2D and 3D dynamic analyses are also similar due to plain strain conditions as shown in Fig. 15. Although a time-varying wave force was applied to the structure, the difference between the minimum and maximum displacements developed was minimal (≈ 0.01mm). This might be due to the low magnitude of the wave force. The vertical settlement was maximum behind the structure with a magnitude of -72mm. No upheaval was observed in the seabed indicating a more realistic output compared to pseudo-static loading. The axial force in the soil anchor due to dynamic loading was 41kN in the 2D model and 48kN in 3D. These forces are slightly higher than that of the pseudo-static analysis results. An exaggerated deformed shape of the structure is shown in Fig. 16.

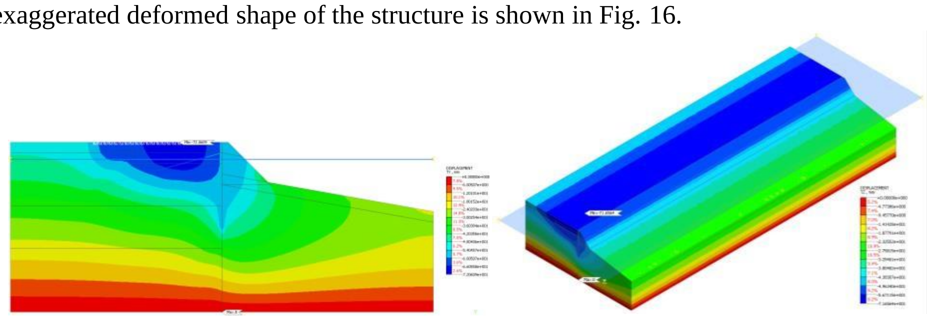

(a) 2D Model (b) 3D Model

Fig. 15. Vertical displacement contour mapping after dynamic analysis

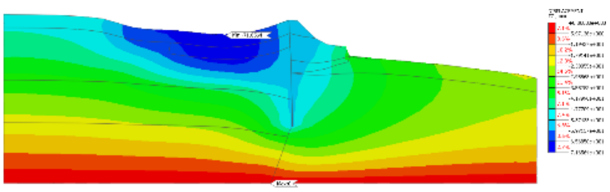

Fig. 16. Deformed shape of the structure post dynamic analysis

5 CONCLUSIONS

The two-lane undivided road and protecting gabion wall near Shankumugham beach in Thiruvananthapuram was washed away due to coastal erosion. The beach road was re-instated by the construction of an 8m deep diaphragm wall with one layer of soil anchor and rubble mound facing. In the present study, 2D and 3D FEM model of the structure were developed and simulated for various construction stages under static and dynamic loading conditions. The obtained stability analysis output was also compared with the 2D LEM results. The following are the important conclusions derived from the study.

a. For the stability analysis in static condition, 2D FEM produced slightly critical results, whereas the 3D FEM results were comparable with the 2D LEM output. The factor of safety values varied inversely with the scour depth of the beach.
b. Due to the plain strain condition, the shear stress and displacement contour in the 3D and 2D models were similar. In Stage 3 and Stage 4, due to anchor prestressing, distress was observed near the pavement layer. A similar observation was made at site during the construction phase.
c. In 2D and 3D models, the dynamic analysis developed higher vertical settlement than the static case. Similarly, higher axial force in soil anchor was found in dynamic analysis, but within the permissible limit.
d. The 2D LEM and 2D & 3D FEM analysis outputs are in good agreement with each other, verifying the safety of the structure for the analyzed conditions.

References

1. BMPTC (Building Materials and Technology Promotion Council) report: Flood hazard map of India. https://bmtpc.org/DataFiles/CMS/file/VAI2019/MAP/floodmap/flood_jpg/ Flood-INDIA.jpg. (2019) Accessed 29 Dec 2019.
2. Davis, R. A. Jr., FitzGerald, D. M.: Beaches and coasts. John Wiley & Sons, Hoboken (2009).
3. Deo, M. C.: Waves and structures. Mumbai. Indian Institute of Technology Bombay (2013).
4. Erlandson, J. M.: As the world warms: rising seas, coastal archaeology, and the erosion of maritime history. Journal of Coastal Conservation, 16(2), 137–142 (2012).
5. Fowler, J. E.: Coastal scour problems and methods for prediction of maximum scour. In: US Army Corps of Engineers. Technical Report CERC, Washington, 93–98 (1993).
6. IRC 75: Guidelines for the design of high embankments. Indian Roads Congress, New Delhi (2015).
7. IS 9556: Code of practice for design and construction of diaphragm walls. Bureau of Indian Standard, New Delhi (2003).
8. IS 10270: Guidelines for design and construction of prestressed rock anchors. Bureau of Indian Standard, New Delhi (2003).
9. Sreekantan, P. G., Sinha, A. K., Havanagi, V. G., Dayana, M.: Failure analysis and mitigation of Shankumugham beach road, Kerala, India-a case study. Arabian Journal of Geosciences 15, 1263 (2022).
10. Vishnu, C. L., Sajinkumar, K. S., Oomen, T., Coffman, R. A., Thrivikramji, V. R., Rani, V. R., Keerthy, S.: Satellite-based assessment of the August 2018 flood in parts of Kerala, India. Geomatics, Natural Hazards and Risk 10(1), 758–767 (2019).